Supplementary Materials
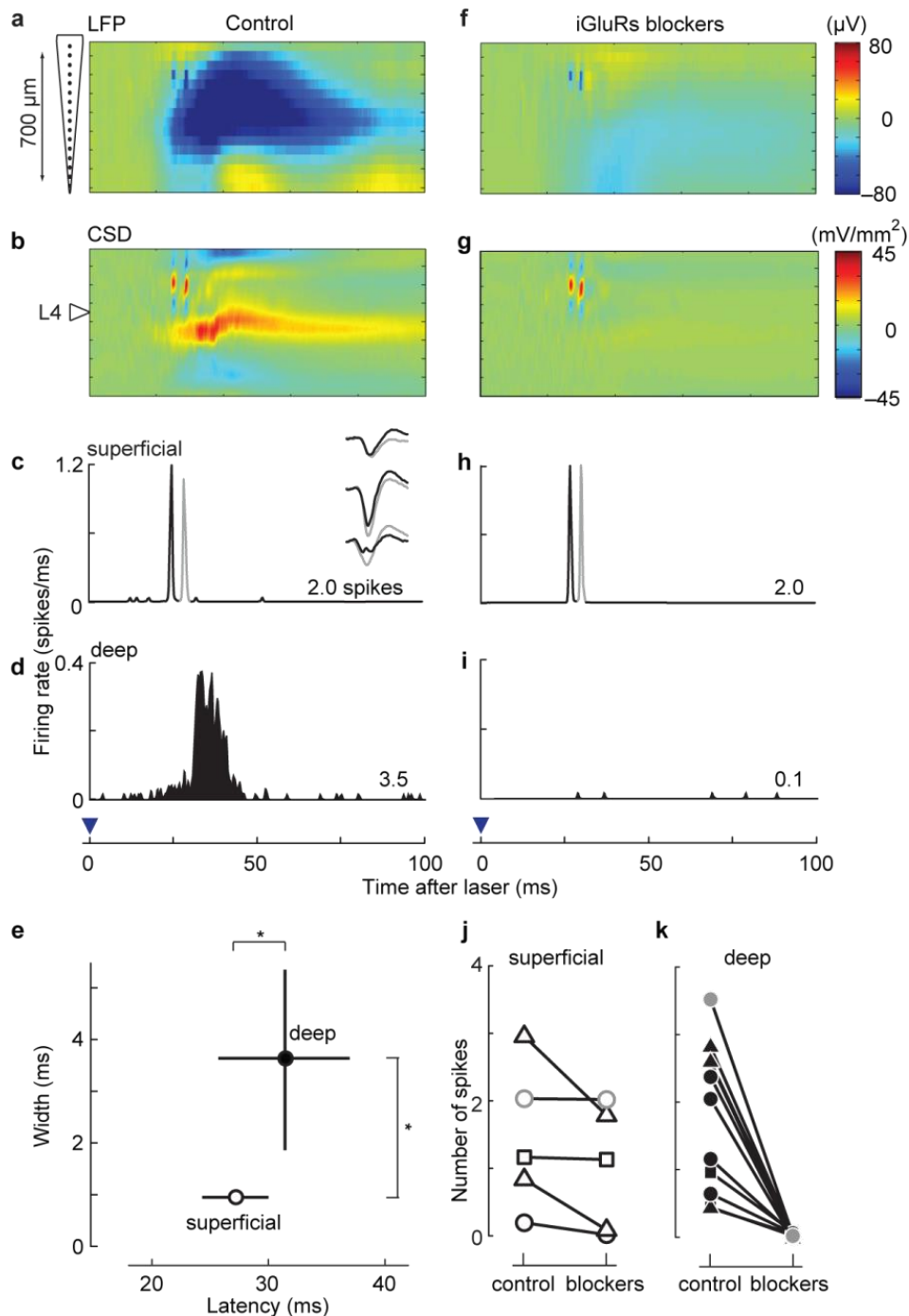
**Supplementary Figure 1.** Optogenetic antidromic stimulation: physiology and pharmacology. Data are as in Fig. 1g,h. (a) LFP response to callosal laser stimulation, measured along cortical depth (700 μm, inset). Note no negative deflection for the initial 20 ms, indicating no effect of stray light from the optic stimulus. (b) Corresponding CSD profile. Arrow indicates estimated position of L4. (c) Firing rate histograms from a superficial layer. Bin width was 125 μs. The two peaks are from two different neurons (inset show their spike shapes). The number of spikes per stimulus is on bottom right. (d) Same, for a deep layer. (e) Half-width vs. onset latency of firing rate responses (superficial layers n = 14, deep layers n = 30). Onset latency for superficial layers (27.1 ± 2.9 ms, n = 14) gives an estimation of axonal conduction velocity as 0.37 m/s, within the reported range (0.3–12 m/s, Swadlow, H.A., and Waxman, S.G., *Experimental Neurology* 53:128-150, 1976). (f-i) Same as a-d, in the presence of iGluR blockers (CNQX, D-AP5, 2 mM respectively). (j,k) Effect of iGluR blockers on spike activity in three animals. Different symbols indicate different animals. Open gray circles are from c and h, and closed circles from d and i.
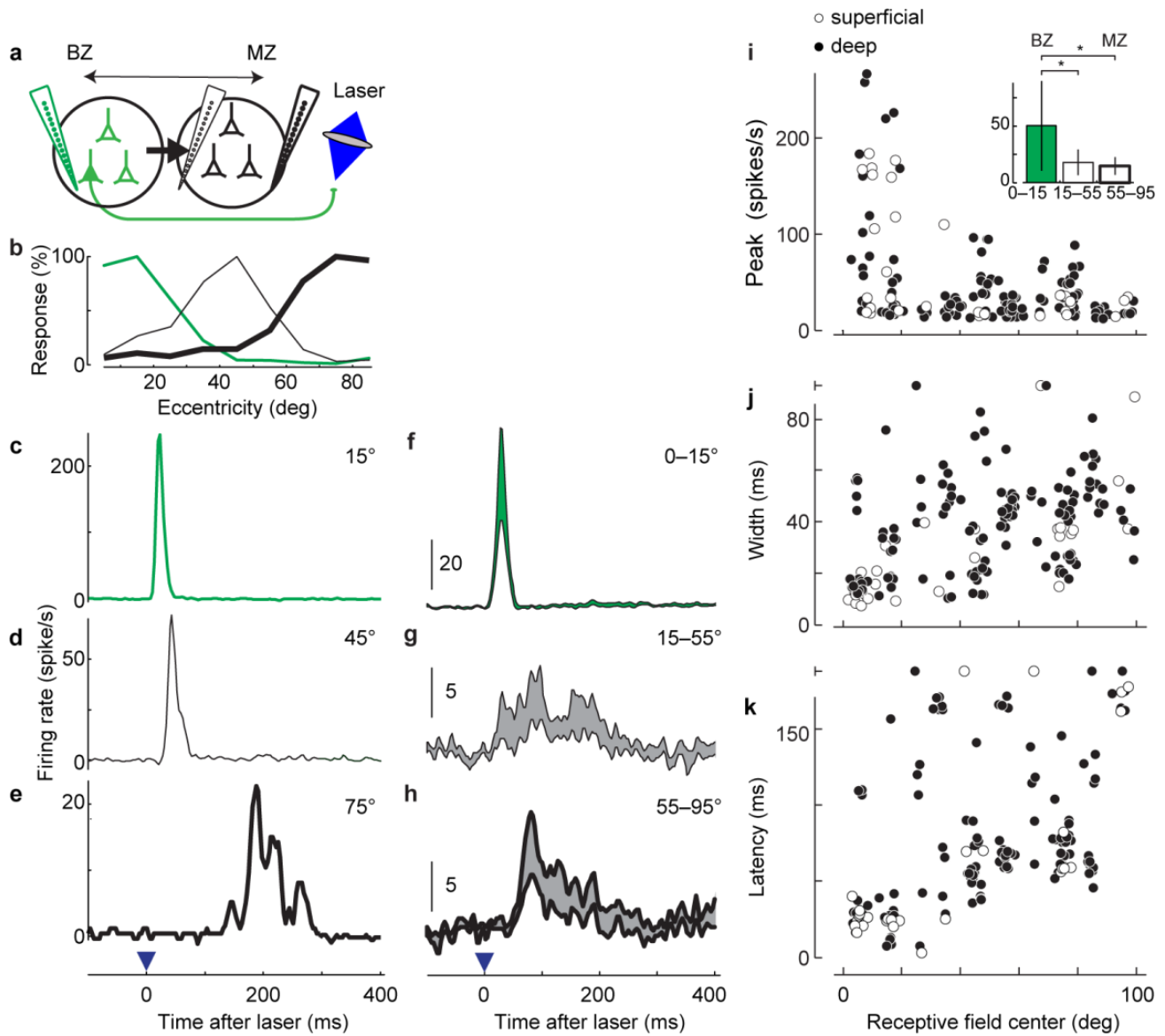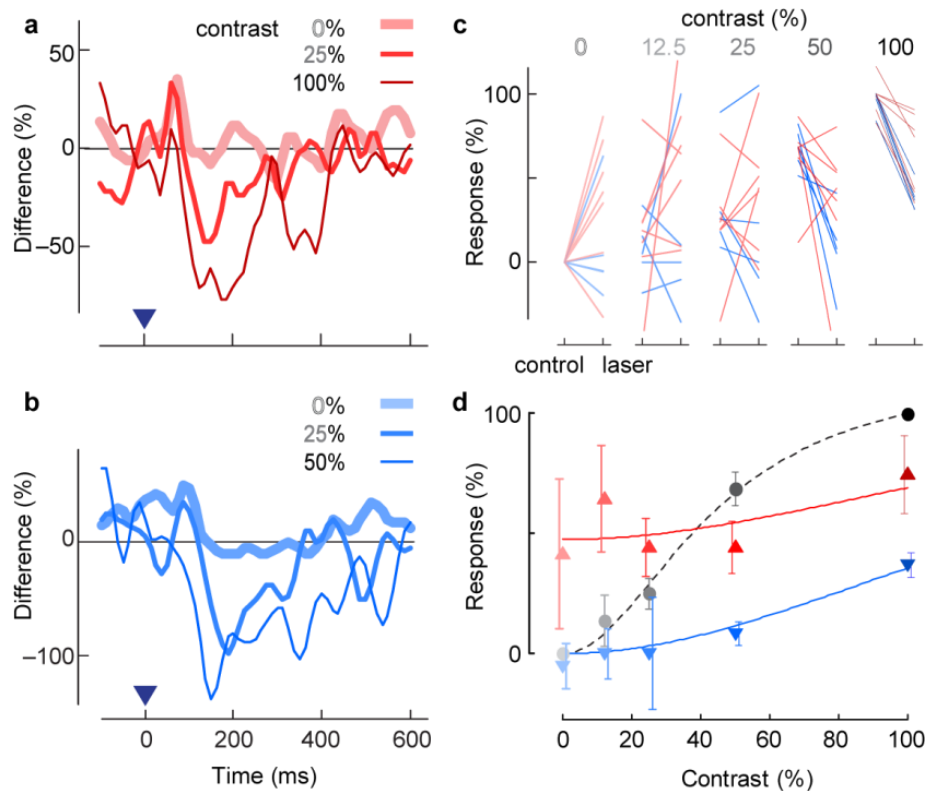
Supplementary Figure 2. Distal activation in the absence of visual stimuli. (a) Silicon probe electrodes were placed in the binocular zone (BZ) and/or in the monocular zone (MZ). Activity in the BZ was elicited antidromically through contralateral laser stimulation. (b) Selectivity for retinotopic position of three units recorded simultaneously with multi-shank electrodes (shank spacing 400 µm), in BZ (green), and in MZ (black). (c) Firing rate responses of the BZ unit to callosal stimulation. Bin width was 12.5 ms. (d,e) Same, for the MZ units (recorded simultaneously). Note different vertical scale. (f-h) Averaged firing rate response for three the retinotopic positions. Activity was averaged first among units on the same shank, then among all the shanks within the same retinotopic position (callosal BZ: n = 9 shanks from 19 animals, acallosal BZ- near MZ: n = 11, far MZ: n = 14). Shaded areas indicate standard error of mean. Scale bars are in spikes/s. (i-k) For units where activation was significant, we measured the activation peak (the maximum of the response curve, i), half width (the duration when the response curve was above 50% of the peak, j) and onset latency (the first time when the response curve reached 50% of the peak, k). Open circles are for units in superficial layers, and closed circles for units in deep layers. To make all data points visible, a small random fluctuation was imposed on the horizontal position of each data point. The activation peak was significantly larger in callosal BZ ((i) inset, n = 44, p < 0.05, Mann-Whitney test) than in acallosal BZ-near MZ (n = 45) or in far MZ (n = 76).
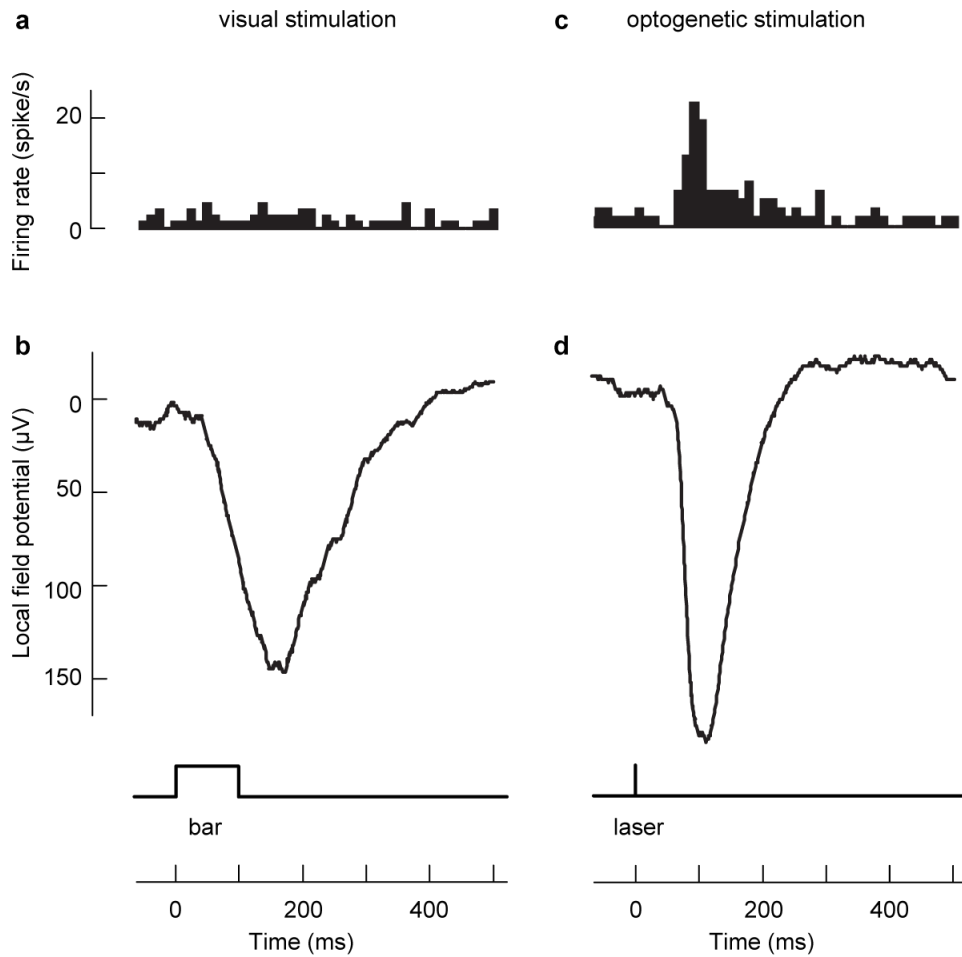
Supplementary Figure 3. Comparison between optogenetic stimulation and distal visual stimulation. The recording site lies in a deep layer of V1 in the far MZ (RF center = 65°), and the response was averaged across > 50 repeats. (a-b) Spike activity and LFP activity following a flash of a bar presented binocularly on the vertical meridian (0–30°) to drive the BZ visually. (c-d) Same, for the activity following optogenetic stimulation of callosal neurons in the BZ. They were confirmed in all 2 mice.
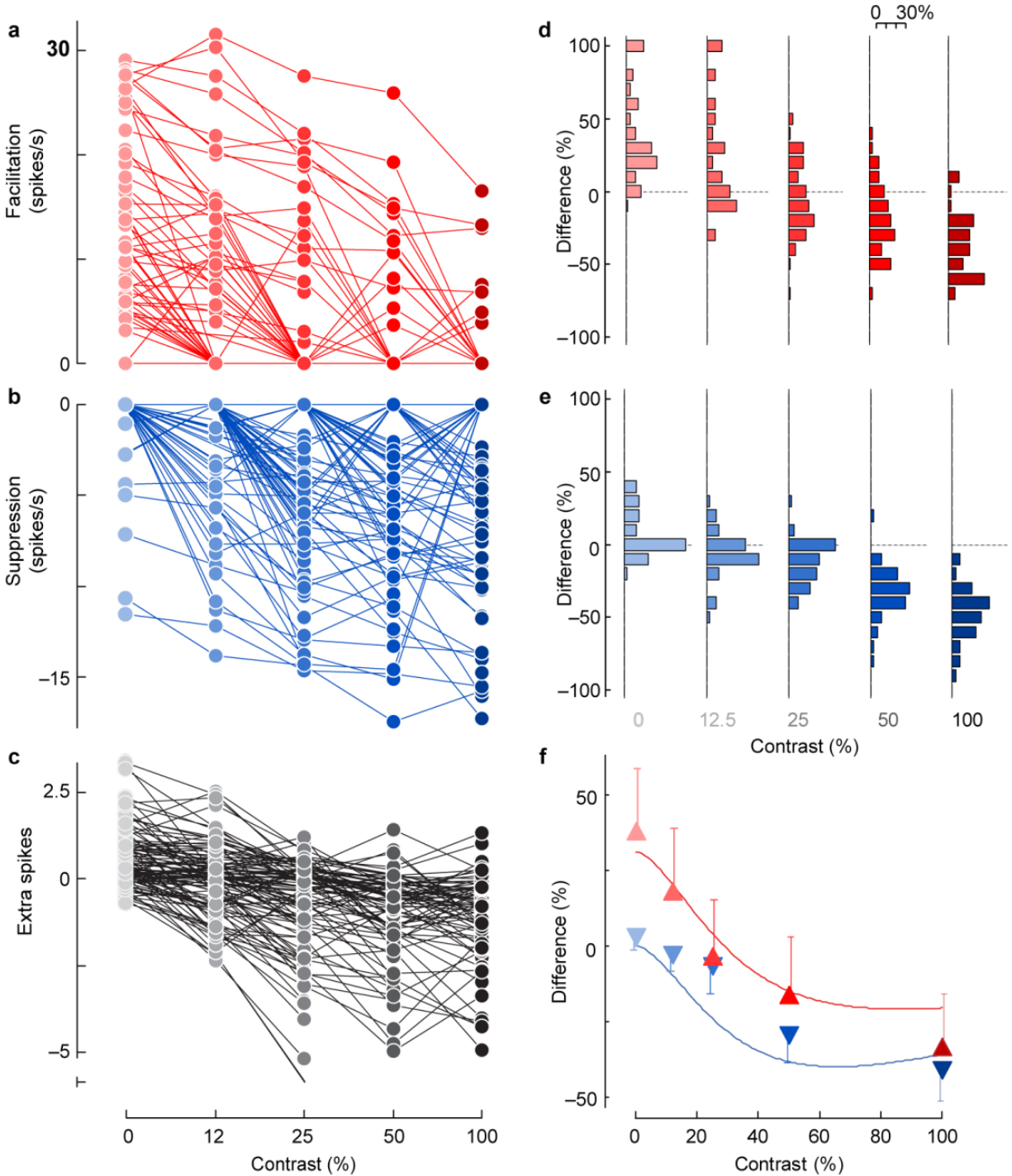
Supplementary Figure 4. Contrast-dependent effects of distal activation in the far MZ. (a-c) Panels show the effects on the activation peak (a, n = 56), on the suppressive peak (b, n = 103), and on the overall spike count change in a 600 ms window following laser stimulation (c, n = 103). (d-f) Histograms measure the difference in normalized response between control and laser stimulation (data shown in Fig.4g). (d) Sites with activation and suppression (n = 56). (e) Sites with suppression alone (b, n = 47). (f) The population response as a function of stimulus contrast, for sites with activation and suppression (red) and sites with suppression alone (blue). The curves illustrate the prediction based on the normalization model, using the same set of parameter values as in Fig. 3a,b.

5

Supplementary Figure 5. Confirmation of the main results with isolated units. (a) The difference in firing rate between control and laser conditions for an example unit that showed activation and suppression (normalized as described in Methods). RF center 55°. (b) Same analysis, for an example unit that showed no activation at 0% contrast, only increasing suppression with increasing contrast. (c) Normalized response measured from 50 to 250 ms at various contrasts in the absence (control) and the presence (laser) of distal activation. Red points are units with activation and suppression (n = 7) and blue with suppression alone (n = 5). (i) The median values in panel c plotted as a function of stimulus contrast. Three curves indicate the fit of the normalization model (Eq. 1), using a single set of parameter values.
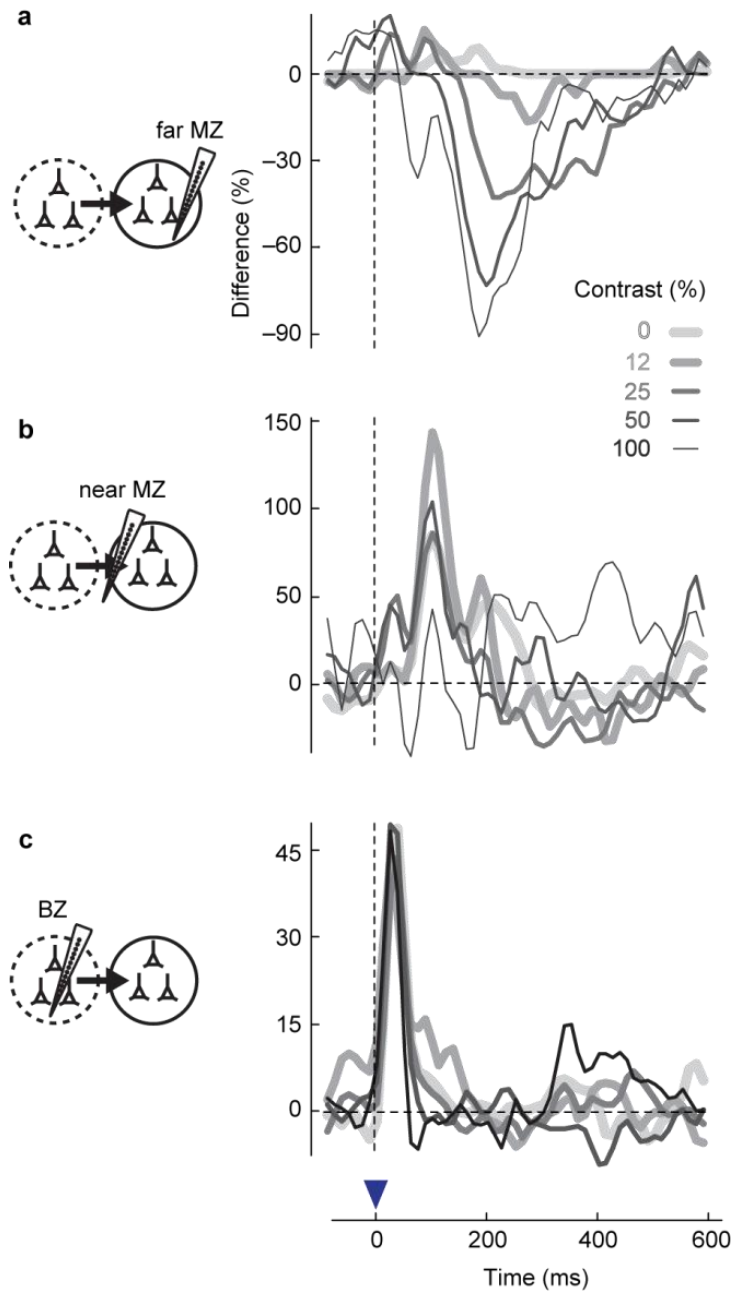
Supplementary Figure 6. Effects of optogenetic stimulation as a function of space and of stimulus contrast. (a)Averaged normalized response for all units with significant activation or suppression in the far MZ (55–95° eccentricity, n = 103 units). Responses are scaled relative to r_{100}. (b) Average of 41 units in the near MZ (30–55°). Scaling is relative to r_{25}, as 25% contrast is the stimulus condition included in all experiments. (c) Average of 15 units in BZ (0–30°). These neurons were located in the deep layers, so they were not antidromically activated. Scaling is relative to the peak firing rate in response to callosal stimulation at 0% contrast. Different units had different peak time, resulting in a smaller peak than 100%.
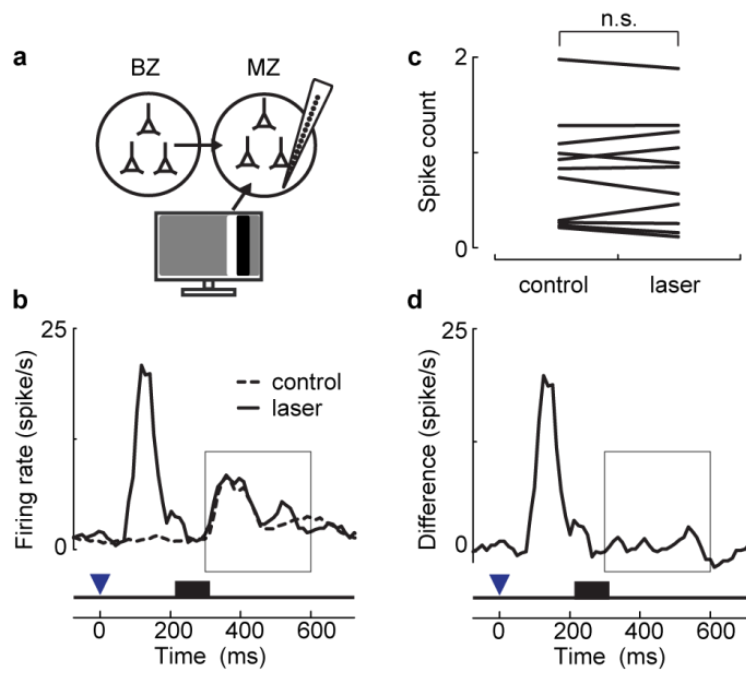
Supplementary Figure 7. Activation is not followed by suppression. (a) a flash of grating bars was presented in the monocular visual field after optogenetic stimulation of distal sites. (b) Firing rate responses of one example MZ neuron to visual stimulation alone (dotted line) or to visual stimulation preceded by distal activation (solid line). A blue arrow and a black square indicate the timing of laser and visual stimulation. The difference in firing rate between two conditions is shown in d. (c) Spikes occurring between 300 and 600 ms (a squared range) were counted for 11 units (2 animals). There was no statistical difference (control: 0.82 ± 0.47, laser: 0.84 ± 0.38, p > 0.05, Wilcoxon test).
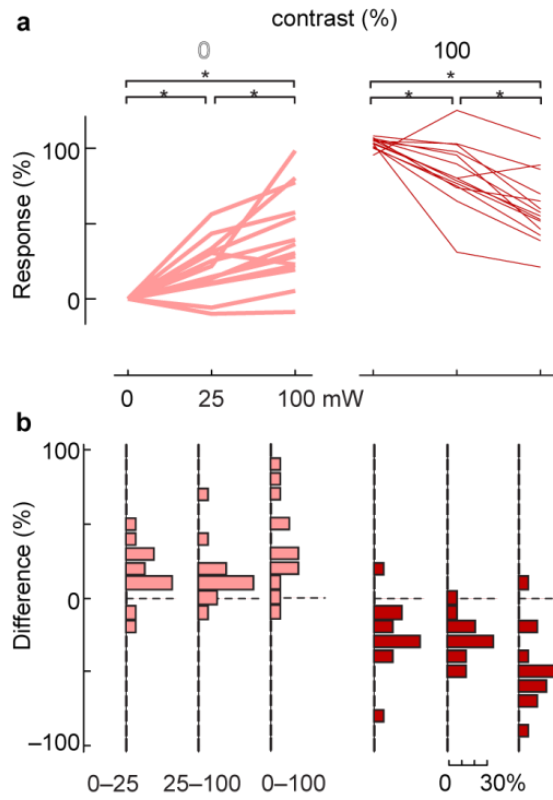
Supplementary Figure 8. Effects of laser power on activation and suppression. (a) Normalized response at 0% and 100% contrasts in the absence (control) and the presence (25 mW or 100 mW) of laser stimulation for units showing both activation and suppression (n = 14). Statistical significance was tested with Wilcoxon text (p < 0.05). (b) Difference among three conditions was measured and shown in bar plots (n = 14).

	Callosal BZ				Acallosal BZ				Near MZ				Far MZ			
	all	A	S	A+S	all	A	S	A+S	all	A	S	A+S	all	A	S	A+S
Superficial	30	13	0	1	5	1	0	0	15	4	0	0	34	10	0	0
	3	0	0	0	0	0	0	0	12	4	1	2	19	0	5	9
Deep	45	30	0	0	10	5	0	0	62	32	1	3	163	59	5	7
	14	13	0	0	8	2	0	0	41	11	12	11	113	0	42	47
Total	75	43	0	1	15	6	0	0	77	36	1	3	197	69	5	7
	17	13	0	0	8	2	0	0	53	15	13	13	132	0	47	56

Supplementary Table. Summary of all the recordings. We recorded from 364 units and we divided them in four groups according to retinotopic position: callosal BZ (0–15° eccentricity), acallosal BZ (15–30°), near MZ (30–55°), and far MZ (55–90°). We further divided them into superficial (layers 2/3 and 4) and deep (layers 5 and 6). The table indicates whether optogenetic stimulation of the BZ activated the units (A), suppressed them (S), or had both effects (A+S). For each condition we indicate the number of units recorded in the absence of visual stimuli (top, 19 mice), and the subset of those that were also recorded in the presence of visual stimuli (bottom, 10 mice).